GSA DATA REPOSITORY 2013281

Data repository for Slab flattening trigger for isotopic disturbance and magmatic flare-up in the southernmost Sierra Nevada batholith, California

Alan D. Chapman*, Jason B. Saleeby, and John Eiler
Division of Geological and Planetary Sciences, California Institute of Technology, Pasadena, California, USA

*Current address: Department of Geosciences, University of Arizona, Tucson, Arizona, USA
E-mail: adchapman@email.arizona.edu.

APPENDIX DR1: Sample Locations, Petrography, and Zircon Morphology

Descriptions of analyzed zircon grains and the samples (corresponding to Fig. 1) from which they were extracted are given below.

Plutonic Rocks

6 (originally 08SE451; 34° 52' 24.2" N, 119° 6' 40.7" W)

Antomony Peak tonalite (Chapman and Saleeby, 2012). Light gray, medium- to coarse-grained, porphyritic, massive to penetratively foliated, hornblende-biotite tonalite containing mainly plagioclase, quartz, and hornblende, with minor amounts of garnet, K-feldspar, biotite, epidote, apatite, titanite, and ilmenite. Where hypidiomorphic granular (igneous) textures are not overprinted by metamorphic foliation, the epidote occurs as subhedral replacement products of embayed hornblende and retains distinct core and rim regions, consistent with a magmatic origin. Original petrographic relationships are locally obscured by extensive seritization and chloritization. Hornblende-rich mafic schlieren are found in the same outcrop as 08SE451. See Chapman et al. (2012) for U-Pb zircon geochronologic data.

7 (originally 08SE46; 34° 54' 35.3" N, 118° 58' 30.7" W)

San Emigdio tonalite (Chapman and Saleeby, 2012). Gray, medium- to coarse-grained, weakly foliated biotite tonalite. Alteration is minor. See Chapman et al. (2012) for U-Pb zircon geochronologic data.

8 (originally 08SE675; 34° 53' 48.8" N, 118° 55' 20.9" W)

San Emigdio tonalite (Chapman and Saleeby, 2012). Foliated garnet-biotite leucotonalite. Similar in appearance to the 101 Ma "Garnet-biotite tonalite of Grapevine" of Pickett and Saleeby (1993, 1994). Epidote phenocrysts embayed in biotite. Garnet is 0.5-1 mm in diameter with blebby quartz inclusions. Accessory minerals include zircon, apatite, and opaques. Very little alteration. Radiation-damage halos surrounding zircon inclusions in biotite are common. See Chapman et al. (2012) for U-Pb zircon geochronologic data.

Zircon grains in samples 7 (Fig. DR1a and b), 6 (Fig. DR1c), and 8 (Fig. DR1d) are generally subhedral, ~50 – 350 μm in length, inclusion-poor, and exhibit simple oscillatory zoning patterns in Cathodoluminescence (CL) images that we interpret as magmatic features. Cathodoluminescence-dark cores are commonly overgrown by CL-bright rims up to ~35 μm wide. In situ laser ablation multicollector inductively coupled mass spectrometry analyses of core and rim regions are concordant with weighted mean ages of ca. 134 to 136 Ma and 98.1 ± 4.9 Ma, respectively (Chapman et al., 2012). These ages are interpreted to reflect the timing of crystallization (cores) and deep crustal overgrowth (rims). A single aberrant grain in sample 8, yielding an age of 485.0 ± 34.0 Ma, is interpreted as related to source inheritance and/or entrainment of a Paleozoic or older zircon.

San Emigdio Schist

The San Emigdio Schist is juxtaposed against plutonic rocks along the remains of a locally ductile to brittle low-angle detachment fault system that probably correlates with the type Rand fault exposed in the Rand Mountains (Postlethwaite & Jacobson, 1987). During Pliocene–Quaternary compression, the Rand fault in the San Emigdio Mountains was largely folded with a major south-dipping thrust fault cutting across the folded structural section. Reported sample depths were approximated based on metamorphic grade and the structural distance from the Rand fault in locations where ductile fabrics are well-preserved.

1 (originally 08SE467; 34° 54' 29.3" N, 118° 58' 39.2" W)
San Emigdio Schist metasandstone collected adjacent to the Rand fault. Outcrop contains abundant deformed quartzofeldspathic (milky quartz + plagioclase ± garnet ± muscovite) veins and stromatic leucosomes and melanosomes, interpreted to result from fluid-saturated partial melting (Chapman et al., 2011). Sample is a coarse-grained garnet + plagioclase + biotite + quartz + ilmenite blastomylonitic schist. Garnet porphyroblasts are typically 2 to 4 mm in diameter and subhedral, with inclusions of plagioclase, biotite, and quartz. Diffusive relaxation of major and trace element growth zonation is common in garnet porphyroblasts from this sample. Plagioclase porphyroblasts are twinned, contain little to no graphite and/or carbonaceous material, and exhibit distinct core and rim regions. Quartz grains lack undulatory extinction and display 120˚ grain boundaries. Minor minerals include apatite, zircon, and rutile. Secondary minerals, including clinozoisite, celadonitic muscovite, and fibrolitic sillimanite, usually occur within or adjacent to biotite. Radiation-damage halos surrounding zircon inclusions in biotite are common. Phase relations suggest that peak temperatures exceeded 700˚ C at 10 kbar (Chapman et al., 2011).

2 (originally 99-57 (Grove et al., 2003); 34° 52' 12.6" N, 119° 6' 34.7" W)
San Emigdio Schist metasandstone collected ~25 m below the Rand fault. This sample shows a protomylonitic texture (Grove et al., 2003).

3 (originally 06SE23 and SE1b (Jacobson et al., 2011); 34° 52' 56.0" N, 119° 4' 21.1" W)
San Emigdio Schist metasandstone collected from ~30 m below the Rand fault. Medium- to coarse-grained garnet + plagioclase + biotite + quartz + rutile blastomylonitic schist. Garnet grains are idioblastic and 0.5 to 2 mm in diameter with well-defined growth zonation and blebby inclusions of exclusively quartz confined to individual zones (Chapman et al., 2011), suggesting epitaxial growth of quartz. Some porphyroblasts have pressure shadows composed of fine quartz, plagioclase, and chlorite. Some garnet grains are torn completely apart or frictionally displaced up to 2 mm along fractured surfaces with no systematic orientation. Plagioclase is poikiloblastic with blebby quartz inclusions and finely disseminated graphite and/or carbonaceous material. Some grains exhibit polysynthetic twinning. Quartz grains lack undulatory extinction and display 120˚ grain boundaries, indicative of high-temperature annealing. Secondary alteration is mainly restricted to mm-scale shear bands that truncate the peak mineral assemblage and contain retrograde clinozoisite, chlorite, celadonitic muscovite, and tourmaline. Sample contains minor tschermakitic hornblende. Calculated temperatures and pressures for this sample are 665 ± 29 °C and 10.0 ± 0.9 kbar (Chapman et al., 2011).

4 (originally SE03 (Jacobson et al., 2011); location approximate: 34° 52' 51.2" N, 119° 3' 21.6" W)
San Emigdio Schist metasandstone collected from ~100 m below the Rand fault.

5 (originally 07SE34; 34° 53' 4.4" N, 119° 1' 38.4" W)
San Emigdio Schist metasandstone collected from ~400 m below the Rand fault. Fine- to medium-grained plagioclase + biotite + chlorite + muscovite + clinozoisite + quartz granular schist. A faint shape-preferred orientation of biotite defines the schistosity. Plagioclase is poikiloblastic, lacks twinning, and

contains blebby quartz inclusions and finely disseminated graphite and/or carbonaceous material. Garnet porphyroblasts are sparse, with a single ~ 1 mm skeletal grain in thin section. Biotite is closely associated with ilmenite, tourmaline, and calcite. This sample was not suitable for thermobarometric work since garnet was not in textural equilibrium with plagioclase, biotite, or muscovite. However, phase relations suggest that peak temperatures did not exceed 600 ˚C (Chapman et al., 2011).

Zircon grains from all structural levels in the schist share similar morphologies. Most grains are subhedral to anhedral, ~ 10 – 150 μm in length, inclusion-poor, with abundant fractures. Cathodoluminescence imaging indicates a clear relationship between zircon zoning patters and structural depth (Fig. DR1). At the deepest levels of exposure (> 100 m; e.g., sample 5; Fig. DR1f), zircons typically exhibit simple oscillatory zoning patterns that we interpret as magmatic features. At shallow structural levels (< 100 m), oscillatory zoning is still generally present; however, metamorphic domains truncate older magmatic zoning in several grains and narrow (1 -50 μm) rims of CL-bright zircon commonly crosscut zoning in zircon cores. Adjacent to the Rand fault (e.g., samples 3; Fig. DR1e and 1; Fig. 2), little to no oscillatory zoning is present in zircons; instead, zircons lack cores and display complex metamorphic zoning patterns characterized by multiple crosscutting domains.

APPENDIX DR2: Analytical Methods

Laser Ablation–Multicollector Inductively Coupled Plasma–Mass Spectrometry

U-Pb geochronology of zircon grains was conducted by laser ablation multicollector inductively coupled plasma mass spectrometry (LA-MC-ICPMS) at the Arizona LaserChron Center following the methods outlined in Gehrels et al. (2006). Zircon grains were extracted from plutonic and metamorphic samples using standard mineral separation techniques of crushing, sieveing, magnetic separation, processing through heavy liquids, and hand picking. Separates were then mounted in epoxy, polished, and imaged on the Caltech Zeiss 1550 VP field emission scanning electron microscope before analysis. Representative CL images are shown in Figure DR1. Zircons were ablated using a 193 nm ArF laser with a pit depth of ~12 μm and spot diameters of 25-30 μm depending on grain size. SL2 (564 Ma ± 4 Ma; Gehrels, personal communication, 2011) and R33 (419 ± 1 Ma; Black et al., 2004) zircon standards were used. Data reduction was done using in-house Arizona LaserChron Center Microsoft Excel programs and ISOPLOT/Ex Version 3 (Ludwig, 2003). U-Pb isotopic data is presented in Table SD1. Plots of U-content and U/Th versus U-Pb age are shown in Figure DR2.

SIMS

Oxygen isotope analyses were conducted with a CAMECA IMS 7f-GEO magnetic sector type secondary ion mass spectrometry (SIMS) instrument at the Caltech Center for Microanalysis. Grain mounts used in U-Pb analysis were polished with 0.25 μm colloidal silica and gold coated prior to SIMS analysis. When possible, zircon grains were analyzed from the same crystal growth domain where U-Pb data were obtained. Zircon grains were sputtered using a 2 nA $^{133}Cs^{+}$ primary ion beam with 20x30 μm diameter, secondary ions were extracted at 10 kV, and $^{16}O^{-}$ and $^{18}O^{-}$ were measured simultaneously using electron multiplier detectors and $^{18}O/^{16}O$ isotope ratios were derived. Each analysis involved 10 to 60 seconds of pre-sputtering, followed by 10 to 20 cycles of data collection, resulting in a total analysis time of 2 to 5 minutes per spot. Instrumental mass fractionation (IMF) was corrected for, using raw isotopic ratios, by bracketing sample and R33 standard (5.55 ± 0.04‰; Valley, 2003) analyses every 5 to 10 measurements. Finally, $\delta^{18}O_{VSMOW}$ values were calculated using IMF-corrected isotopic ratios. The internal precision on each standard analysis based on counting statistics was typically between ±0.25‰ and ±0.8‰ (2σ) and

spot-to-spot reproducibility was typically better than 0.6‰. Oxygen isotope data is presented in Table SD2 and Figures 3 and SD3.

REFERENCES CITED

Black, L. P., Kamo, S. L., Allen, C. M., Davis, D. W., Aleinikoff, J. N., Valley, J. W., Mundil, R., Campbell, I. H., Korsch, R. J., Williams, I. S., and Foudoulis, C., 2004, Improved $^{206}Pb/^{238}U$ microprobe geochronology by the monitoring of a trace-element-related matrix effect; SHRIMP, ID-TIMS, ELA-ICP-MS and oxygen isotope documentation for a series of zircon standards: Chemical Geology, v. 205, p. 115-140.

Chapman, A. D. and Saleeby, J., 2012, Geologic map of the San Emigdio Mountains, Geological Society of America digital map and chart series, MCH-101, 1:40,000 scale.

Chapman, A. D., Luffi, P., Saleeby, J., and Petersen, S., 2011, Metamorphic evolution, partial melting, and rapid exhumation above an ancient flat slab: Insights from the San Emigdio Schist, southern California: Journal of Metamorphic Geology.

Chapman, A. D., Saleeby, J. B., Wood, D. J., , Piasecki, A, Farley, K. A., Kidder, S., and Ducea, M. N., 2012, Late Cretaceous gravitational collapse of the southern Sierra Nevada batholith, California. Geosphere, doi: 10.1130/GES00740.1, v. 8, p. 314-341.

Crowell, J. C., 1952, Geology of the Lebec Quadrangle, California: Special Report - California Division of Mines and Geology, v. 24, p. 1-24.

Dibblee, T. W., Jr., and Nilsen, T. H., 1973, Geologic map of San Emigdio and western Tehachapi Mountains, *in* Vedder, J. G., ed., Sedimentary facies changes in Tertiary rocks-California Transverse and southern Coast Ranges, Society of Economic Paleontologists and Mineralogists guidebook to field trip 2: Anaheim, California.

Gehrels, G., Valencia, V., and Pullen, A., 2006, Detrital zircon geochronology by laser-ablation multicollector ICPMS at the Arizona Laserchron Center: The Paleontological Society Papers, v. 12, p. 67-76.

Grove, M., Jacobson, C. E., Barth, A. P., and Vucic, A., 2003, Temporal and spatial trends of Late Cretaceous-early Tertiary underplating Pelona and related schist beneath Southern California and southwestern Arizona: Special Paper - Geological Society of America, v. 374, p. 381-406.

Jacobson, C. E., Grove, M., Pedrick, J. N., Barth, A. P., Marsaglia, K. M., Gehrels, G. E., and Nourse, J. A., 2011, Late Cretaceous - early Cenozoic tectonic evolution of the southern California margin inferred from provenance of trench and forearc sediments: Geological Society of America Bulletin, v. 123, no. 3-4, p. 485-506.

Ludwig, K. R., 2003, Mathematical-statistical treatment of data and errors for (super 230) Th/U geochronology: Reviews in Mineralogy and Geochemistry, v. 52, p. 631-656.

Pickett, D. A., and Saleeby, J. B., 1993, Thermobarometric constraints on the depth of exposure and conditions of plutonism and metamorphism at deep levels of the Sierra Nevada Batholith, Tehachapi Mountains, California: Journal of Geophysical Research, v. 98, no. B1, p. 609-629.

Pickett, D. A., and Saleeby, J. B., 1994, Nd, Sr, and Pb isotopic characteristics of Cretaceous intrusive rocks from deep levels of the Sierra Nevada Batholith, Tehachapi Mountains, California: Contributions to Mineralogy and Petrology, v. 118, no. 2, p. 198-215, doi: 110.1007/BF01052869.

Postlethwaite, C. E., and Jacobson, C. E., 1987, Early history and reactivation of the Rand Thrust, Southern California: Journal of Structural Geology, **9**(2), 195-205, doi:110.1016/0191-8141(1087)90025-90023.

Ross, D. C., 1989, The metamorphic and plutonic rocks of the southernmost Sierra Nevada, California, and their tectonic framework: U.S. Geological Survey Professional Paper, v. 1381, p. 159 pp.

Saleeby, J., Farley, K. A., Kistler, R. W., and Fleck, R. J., 2007, Thermal evolution and exhumation of deep-level batholithic exposures, southernmost Sierra Nevada, California: Special Paper - Geological Society of America, v. 419, p. 39-66.

Sharry, J., 1981, The geology of the western Tehachapi Mountains, California. Ph.D. thesis, Massachusetts Institute of Technology.

Valley, J. W., 2003, Oxygen isotopes in zircon: Reviews in Mineralogy and Geochemistry, v. 53, p. 343-385.

Wood, D. J., 1997, Geology of the eastern Tehachapi Mountains and Late Cretaceous-early Cenozoic tectonics of the southern Sierra Nevada region, Kern County, California. Ph.D. thesis, California Institute of Technology.

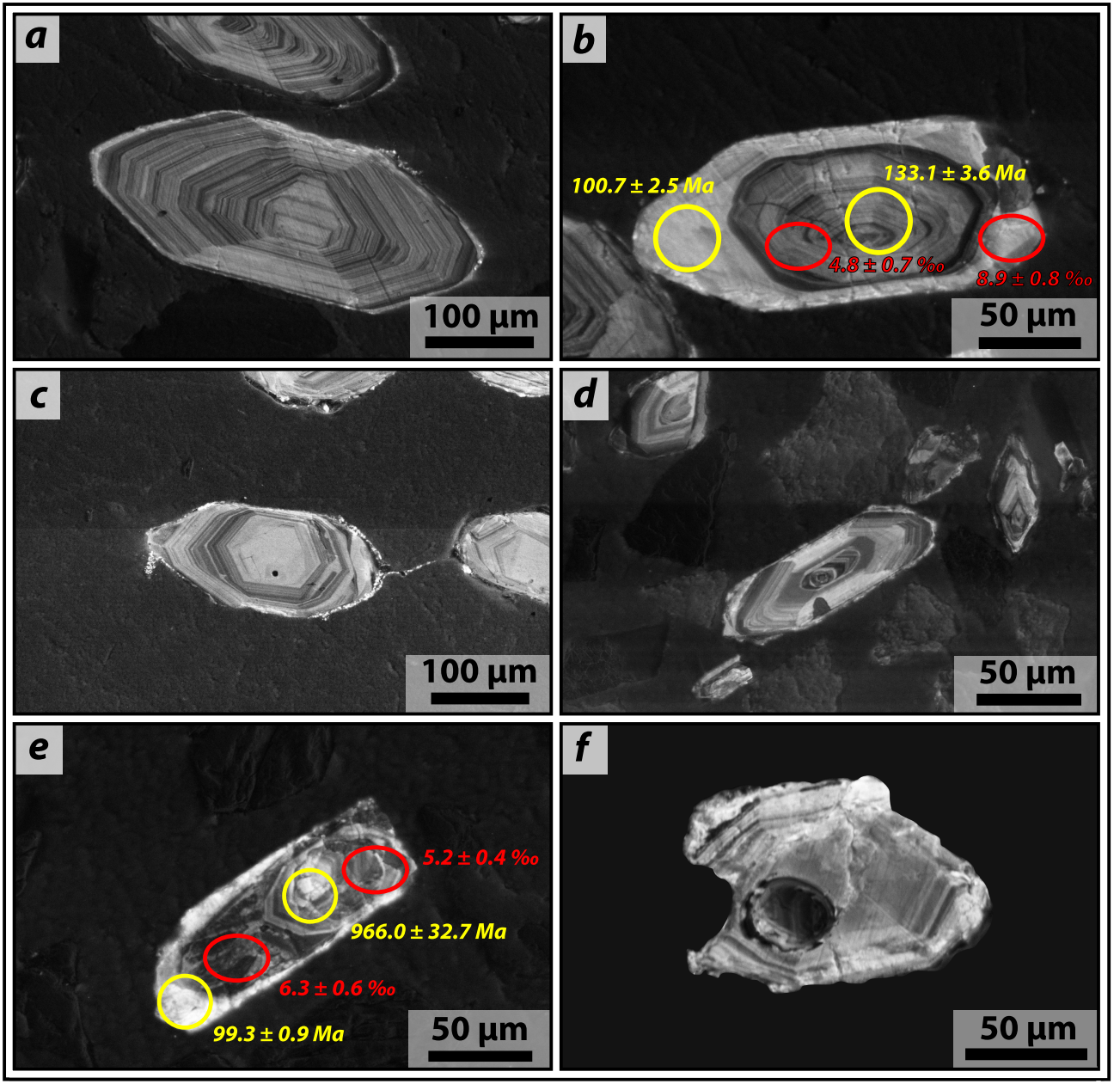

Figure DR1. Supplementary representative cathodoluminescence images of selected zircon grains from upper plate samples 7 (originally 08SE46; a and b), 6 (originally 08SE451; c), and 8 (originally 08SE675; d), and schist samples 3 (originally 06SE23; e) and 5 (originally 07SE34; f). Analysis 06SE23-3b (966.0 ± 32.7 Ma) was included (e) despite being > 30% discordant to illustrate a core-rim age difference. Yellow circles indicate laser ablation multicollector inductively coupled plasma mass spectrometry analyzed areas labeled with 206Pb/238U ages. Red ellipses indicate SIMS analyzed areas labeled with δ18O. All uncertainties are 2σ.

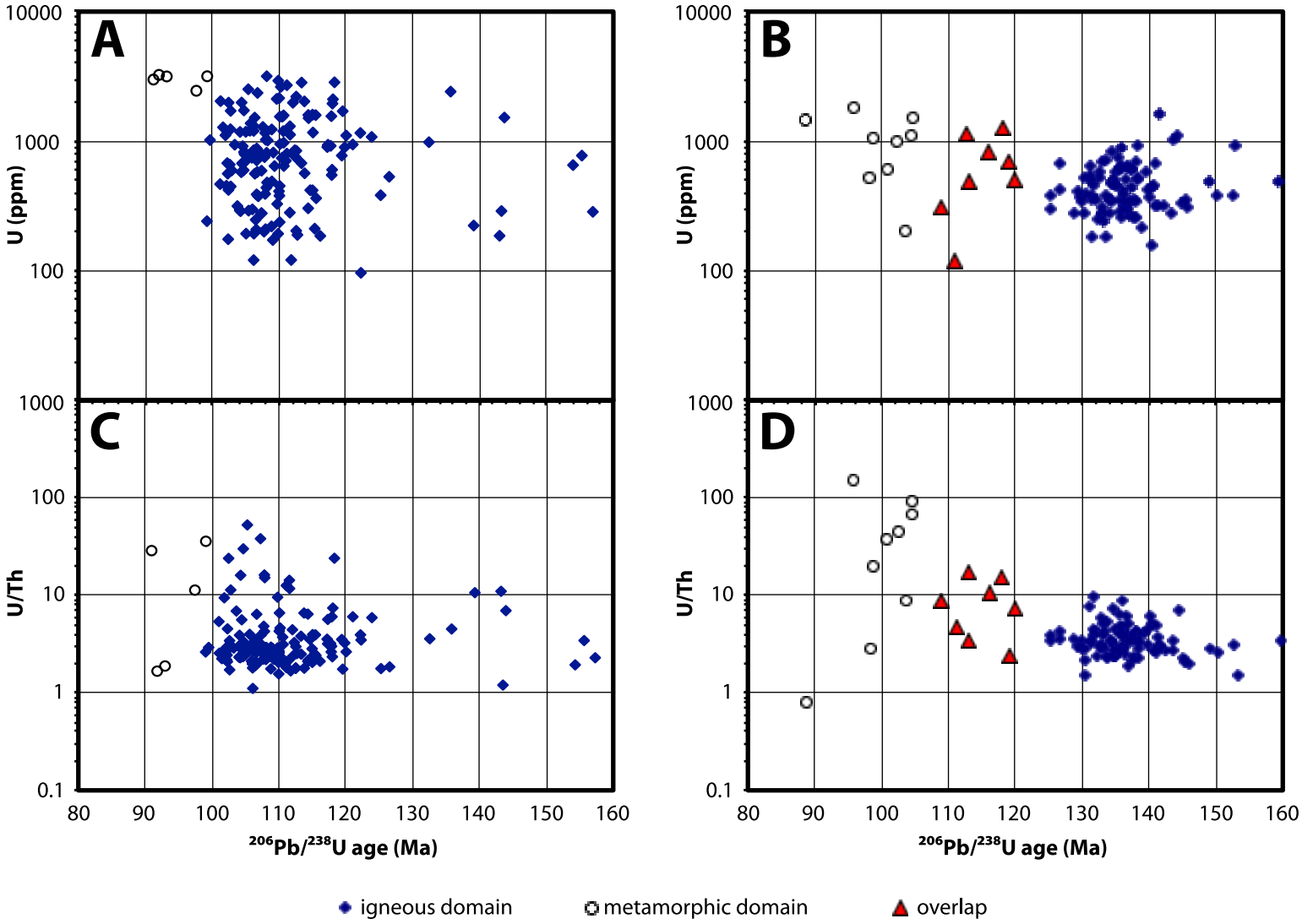

Figure DR2. Plots of zircon trace element chemistry versus U-Pb age for all available data from the San Emigdio Schist (A and C) and upper plate batholithic rocks (B and D). Data from Grove et al. (2003) (original sample 9957), Jacobson et al. (2011) (original samples SE1b and SE03), Chapman et al. (2012) (original samples 08SE46, 08SE451, and 08SE675), and this study (original samples 06SE23, 07SE34, and 08SE467).

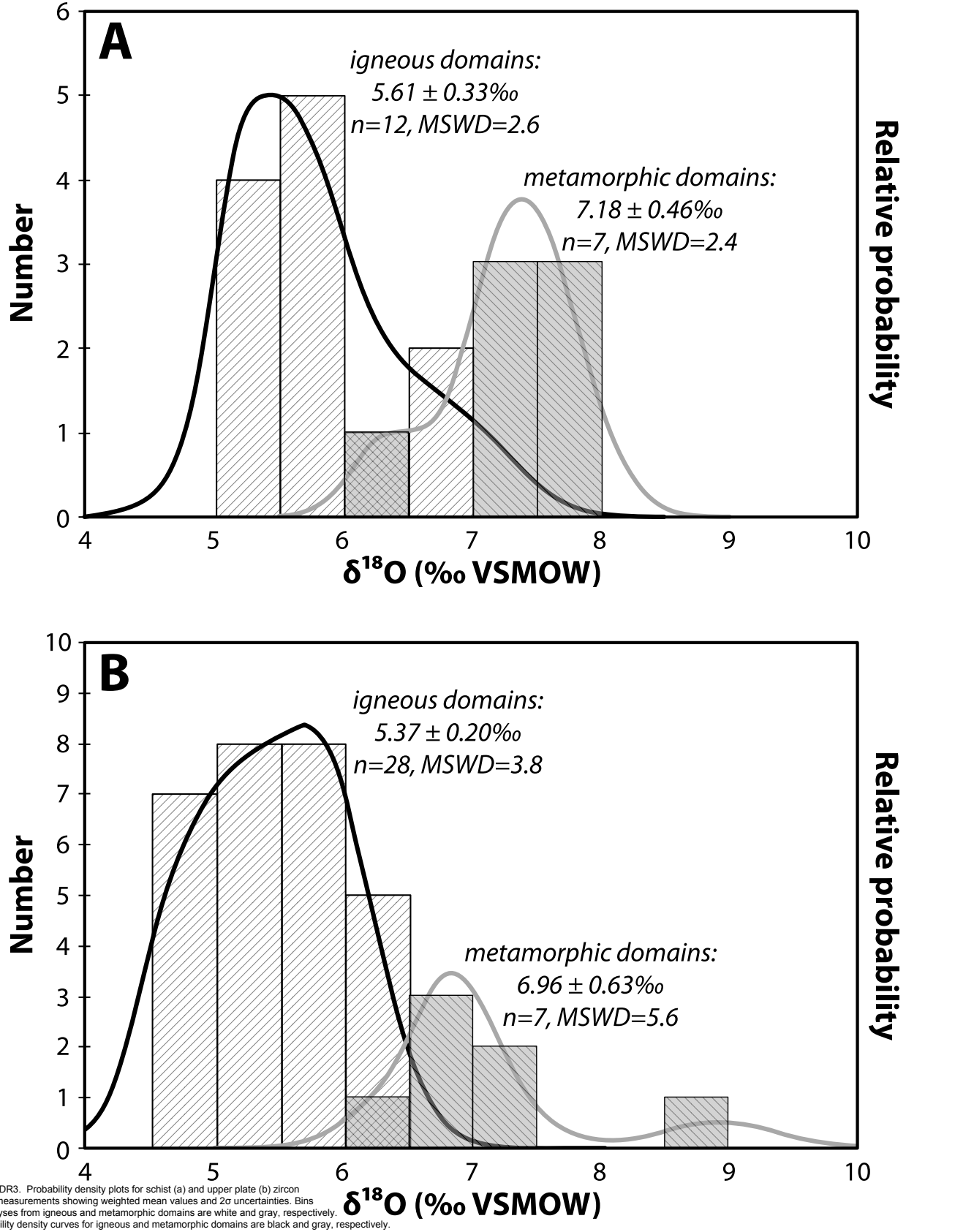

Figure DR3. Probability density plots for schist (a) and upper plate (b) zircon δ18O measurements showing weighted mean values and 2σ uncertainties. Bins of analyses from igneous and metamorphic domains are white and gray, respectively. Probability density curves for igneous and metamorphic domains are black and gray, respectively.

TABLE DR1. Laser ablation multicollector inductively coupled plasma mass spectrometry U-Pb zircon data. Analyses in which epoxy was overlapped and those with greater than 10% uncertainty, 30% discordance, and/or 5% reverse discordance are excluded. Uncertainties given at 1σ.

3 (originally 06SE23) San Emigdio Schist - San Emigdio Mountains

							Isotope ratios						Apparent ages (Ma)					
Analysis	CL notes§	U (ppm)	206Pb 204Pb	U/Th	206Pb* 207Pb*	± (%)	207Pb* 235U*	± (%)	206Pb* 238U	± (%)	error corr.	206Pb* 238U*	± (Ma)	207Pb* 235U	± (Ma)	206Pb* 207Pb*	± (Ma)	Best age† (Ma)	± (Ma)
06SE23-1	IG	322	2642	2.3	22.9228	11.0	0.1033	11.3	0.0172	2.3	0.20	109.7	2.5	99.8	10.7	-131.8	273.5	109.7	2.5
06SE23-3	IG	996	6326	2.6	21.0267	2.3	0.1111	2.6	0.0169	1.3	0.49	108.3	1.4	107.0	2.6	77.3	54.1	108.3	1.4
06SE23-4	IG	585	2044	11.3	17.7175	24.7	0.1253	24.7	0.0161	0.8	0.03	102.9	0.8	119.8	28.0	469.8	554.7	102.9	0.8
06SE23-5	IG	413	960	2.1	19.6723	13.7	0.1123	13.9	0.0160	2.6	0.19	102.4	2.7	108.0	14.3	233.3	317.2	102.4	2.7
06SE23-6	IG	551	4198	2.0	21.6204	4.6	0.1061	5.1	0.0166	2.3	0.45	106.4	2.4	102.4	5.0	10.8	110.4	106.4	2.4
06SE23-7	IG	1158	7110	2.3	20.9772	2.1	0.1071	2.5	0.0163	1.4	0.55	104.2	1.4	103.3	2.4	82.9	48.9	104.2	1.4
06SE23-8	IG	1258	5710	2.2	20.9401	1.7	0.1046	2.1	0.0159	1.1	0.55	101.6	1.1	101.0	2.0	87.2	40.6	101.6	1.1
06SE23-9	IG	298	2122	2.1	20.9322	9.1	0.1179	9.2	0.0179	1.3	0.15	114.4	1.5	113.2	9.9	88.1	216.6	114.4	1.5
06SE23-10	IG	471	5806	2.1	20.4895	2.5	0.1827	2.6	0.0272	0.6	0.21	172.7	0.9	170.4	4.0	138.5	58.7	172.7	0.9
06SE23-11	IG	207	2188	2.5	22.6562	10.5	0.1099	11.4	0.0181	4.3	0.38	115.4	5.0	105.9	11.4	-103.0	259.4	115.4	5.0
06SE23-12	IG	1008	7544	2.3	20.9942	3.0	0.1110	3.5	0.0169	1.8	0.50	108.0	1.9	106.9	3.6	81.0	72.1	108.0	1.9
06SE23-13	IG	288	2720	2.9	22.3426	8.6	0.1005	8.7	0.0163	1.0	0.11	104.1	1.0	97.2	8.0	-68.8	211.0	104.1	1.0
06SE23-14	IG	631	1648	2.2	16.6561	19.8	0.1416	19.9	0.0171	2.5	0.12	109.3	2.7	134.5	25.1	604.9	431.2	109.3	2.7
06SE23-15	IG	662	3096	3.1	20.1821	3.1	0.1116	3.3	0.0163	1.2	0.35	104.5	1.2	107.4	3.4	173.9	72.6	104.5	1.2
06SE23-16	IG	551	5742	1.5	20.6434	5.4	0.1725	6.0	0.0258	2.7	0.45	164.4	4.4	161.6	9.0	120.9	127.2	164.4	4.4
06SE23-17	IG	834	3888	1.8	21.0603	3.0	0.1087	3.0	0.0166	0.6	0.20	106.2	0.6	104.8	3.0	73.6	70.4	106.2	0.6
06SE23-19	IG	189	1124	2.8	22.5703	12.2	0.1050	12.4	0.0172	1.8	0.14	109.9	1.9	101.4	11.9	-93.6	301.1	109.9	1.9
06SE23-20	IG	439	4536	1.7	21.8650	6.1	0.1013	7.6	0.0161	4.5	0.60	102.8	4.6	98.0	7.1	-16.3	147.0	102.8	4.6
06SE23-21	IG	665	5698	2.9	21.0225	2.9	0.1049	3.7	0.0160	2.3	0.62	102.3	2.3	101.3	3.6	77.8	68.9	102.3	2.3
06SE23-22	IG	182	1780	2.1	23.6294	13.0	0.1061	13.2	0.0182	2.4	0.18	116.2	2.8	102.4	12.9	-207.4	326.9	116.2	2.8
06SE23-1b	RXL	3121	12100	36.1	20.3951	3.4	0.1049	3.5	0.0155	1.0	0.27	99.3	0.9	101.3	3.4	149.3	80.1	99.3	0.9
06SE23-4b	IG	119	1353	1.6	14.8844	133.1	0.1621	133.2	0.0175	4.6	0.03	111.8	5.1	152.6	190.8	843.5	641.7	111.8	5.1
06SE23-5b	IG	1161	6730	2.4	20.5962	14.0	0.1100	14.1	0.0164	1.7	0.12	105.0	1.8	105.9	14.2	126.3	331.4	105.0	1.8
06SE23-6b	IG	566	2940	2.2	26.6713	31.2	0.0844	31.3	0.0163	2.1	0.07	104.4	2.2	82.2	24.7	-521.0	852.4	104.4	2.2

5 (originally 07SE34) San Emigdio Schist - San Emigdio Mountains

							Isotope ratios						Apparent ages (Ma)					
Analysis	CL notes§	U (ppm)	206Pb 204Pb	U/Th	206Pb* 207Pb*	± (%)	207Pb* 235U*	± (%)	206Pb* 238U	± (%)	error corr.	206Pb* 238U*	± (Ma)	207Pb* 235U	± (Ma)	206Pb* 207Pb*	± (Ma)	Best age† (Ma)	± (Ma)
07SE34-2	IG	276	4431	2.2	20.9852	6.4	0.1148	6.6	0.0175	1.5	0.23	111.6	1.7	110.3	6.9	82.0	152.2	111.6	1.7
07SE34-1	IG	728	9498	2.2	21.0746	3.4	0.1130	3.7	0.0173	1.4	0.39	110.4	1.6	108.7	3.8	71.9	80.9	110.4	1.6
07SE34-3	IG	3123	14724	2.2	20.5700	2.6	0.1134	3.1	0.0169	1.7	0.55	108.2	1.8	109.1	3.2	129.3	60.3	108.2	1.8
07SE34-4	IG	237	1200	2.6	17.5042	18.0	0.1222	18.0	0.0155	0.7	0.04	99.2	0.7	117.0	19.9	496.5	398.4	99.2	0.7
07SE34-5	IG	551	5355	2.1	20.7458	3.6	0.1063	4.5	0.0160	2.8	0.61	102.3	2.8	102.6	4.4	109.2	84.9	102.3	2.8
07SE34-6	IG	306	76191	1.9	9.3456	1.7	4.6608	2.0	0.3159	1.0	0.52	1769.7	15.8	1760.2	16.4	1749.0	30.8	1749.0	30.8
07SE34-7	IG	118	813	3.0	19.0897	11.0	0.1200	11.2	0.0166	2.0	0.18	106.2	2.1	115.1	12.2	302.2	251.5	106.2	2.1
07SE34-8	IG	146	9960	2.8	13.1960	2.7	1.5150	3.2	0.1450	1.8	0.56	872.9	14.9	936.5	19.8	1089.3	53.6	1089.3	53.6
07SE34-9	IG	268	31269	1.9	9.7414	2.0	3.3767	8.3	0.2386	8.0	0.97	1379.3	99.5	1499.0	64.7	1672.6	36.8	1672.6	36.8
07SE34-10	IG	1215	16287	2.8	20.5994	2.7	0.1075	3.0	0.0161	1.3	0.42	102.7	1.3	103.7	2.9	125.9	64.0	102.7	1.3
07SE34-11	IG	420	9189	2.4	20.6232	5.2	0.1776	5.4	0.0266	1.7	0.30	169.0	2.8	166.0	8.3	123.2	122.2	169.0	2.8
07SE34-12	IG	568	7245	2.6	20.9255	4.0	0.1100	4.2	0.0167	1.3	0.30	106.8	1.3	106.0	4.3	88.8	95.8	106.8	1.3
07SE34-13	IG	1768	1998	4.8	12.3930	5.6	0.5182	6.4	0.0466	3.0	0.47	293.5	8.5	423.9	22.1	1213.9	111.1	293.5	8.5
07SE34-14	IG	372	6039	1.5	22.2197	10.0	0.1069	10.2	0.0172	2.0	0.19	110.1	2.1	103.1	10.0	-55.4	244.8	110.1	2.1
07SE34-15	IG	787	7014	1.8	19.9600	2.8	0.1202	3.1	0.0174	1.4	0.46	111.2	1.6	115.2	3.4	199.6	64.0	111.2	1.6
07SE34-16	IG	740	10149	2.5	20.8734	2.6	0.1163	3.6	0.0176	2.5	0.70	112.5	2.8	111.7	3.8	94.7	60.9	112.5	2.8
07SE34-17	IG	519	6612	2.5	20.8777	5.1	0.1695	5.3	0.0257	1.5	0.28	163.4	2.4	159.0	7.8	94.2	120.8	163.4	2.4
07SE34-19	IG	243	12192	1.3	13.3065	1.1	1.6655	1.9	0.1607	1.5	0.79	960.9	13.2	995.5	11.8	1072.6	22.8	1072.6	22.8
07SE34-20	IG	310	4482	6.9	21.3885	6.1	0.1046	6.2	0.0162	1.0	0.17	103.8	1.1	101.0	6.0	36.7	146.6	103.8	1.1
07SE34-21	IG	480	6117	2.3	21.3551	5.1	0.1100	5.2	0.0170	1.3	0.24	108.9	1.4	106.0	5.3	40.5	121.9	108.9	1.4
07SE34-22	IG	259	3741	2.9	20.6896	7.1	0.1744	7.3	0.0262	1.4	0.19	166.5	2.2	163.2	10.9	115.6	168.3	166.5	2.2
07SE34-23	IG	283	5745	3.9	21.6891	9.7	0.1036	10.6	0.0163	4.3	0.40	104.3	4.4	100.1	10.1	3.2	233.3	104.3	4.4
07SE34-24	IG	94	1521	3.4	20.1872	19.6	0.1308	19.7	0.0192	2.1	0.11	122.3	2.6	124.8	23.1	173.3	460.2	122.3	2.6
07SE34-25	IG	693	8955	1.9	20.7260	3.5	0.1156	3.9	0.0174	1.7	0.43	111.0	1.8	111.1	4.1	111.5	82.3	111.0	1.8
07SE34-26	IG	272	1974	3.9	21.1680	10.2	0.1095	10.3	0.0168	1.0	0.10	107.4	1.1	105.5	10.3	61.4	244.4	107.4	1.1
07SE34-27	IG	558	20424	6.1	18.2572	2.5	0.5228	3.6	0.0692	2.6	0.72	431.5	10.9	427.0	12.6	402.9	56.4	431.5	10.9
07SE34-28	IG	1699	30210	2.3	21.1152	3.8	0.1070	4.4	0.0164	2.2	0.50	104.8	2.3	103.2	4.3	67.4	90.3	104.8	2.3
07SE34-29	IG	444	5244	2.5	20.5106	3.2	0.1073	3.3	0.0160	1.0	0.29	102.1	1.0	103.5	3.3	136.1	74.3	102.1	1.0
07SE34-30	IG	1244	30027	4.1	14.1216	2.1	0.6423	4.8	0.0658	4.3	0.90	410.7	17.2	503.7	19.1	952.0	43.2	410.7	17.2
07SE34-31	IG	592	10155	1.8	19.2593	1.7	0.2985	2.2	0.0417	1.4	0.62	263.4	3.5	265.3	5.2	282.0	40.0	263.4	3.5
07SE34-32	IG	285	3573	2.7	20.7048	5.0	0.1098	5.5	0.0165	2.3	0.42	105.5	2.4	105.8	5.5	113.9	118.0	105.5	2.4
07SE34-33	IG	1299	24888	1.9	20.8026	2.1	0.1101	2.4	0.0166	1.2	0.49	106.2	1.2	106.0	2.4	102.8	50.3	106.2	1.2
07SE34-35	IG	740	8850	4.8	20.8668	7.3	0.1115	7.4	0.0169	0.8	0.11	107.9	0.9	107.3	7.5	95.5	173.4	107.9	0.9
07SE34-37	IG	404	5757	2.5	20.8111	6.7	0.1140	7.1	0.0172	2.4	0.34	110.0	2.7	109.7	7.4	101.8	158.9	110.0	2.7
07SE34-38	IG	200	2202	1.8	21.5126	11.0	0.1129	11.1	0.0176	1.4	0.13	112.6	1.6	108.6	11.4	22.8	263.7	112.6	1.6
07SE34-39	IG	699	4788	3.1	20.2620	2.2	0.1135	2.7	0.0167	1.5	0.56	106.7	1.6	109.2	2.8	164.6	51.6	106.7	1.6
07SE34-40	IG	385	4581	4.2	20.7274	5.2	0.1123	5.4	0.0169	1.7	0.32	107.9	1.9	108.1	5.6	111.3	121.7	107.9	1.9
07SE34-41	IG	381	2475	1.9	13.6054	36.4	0.1691	36.4	0.0167	0.8	0.02	106.7	0.8	158.6	53.5	1027.8	760.3	106.7	0.8
07SE34-42	IG	2375	3060	4.5	15.9218	3.6	0.1843	3.6	0.0213	0.7	0.20	135.7	1.0	171.7	5.7	701.7	75.8	135.7	1.0
07SE34-43	IG	665	8898	3.8	19.7412	9.6	0.1239	9.9	0.0177	2.3	0.23	113.4	2.5	118.6	11.1	225.2	222.6	113.4	2.5
07SE34-44	IG	193	42399	2.7	9.5642	1.8	3.3284	4.5	0.2309	4.1	0.92	1339.1	49.7	1487.7	35.1	1706.5	33.3	1706.5	33.3
07SE34-45	IG	204	6129	1.7	18.0605	2.9	0.5482	4.3	0.0718	3.2	0.74	447.0	13.9	443.8	15.6	427.1	64.6	447.0	13.9
07SE34-46	IG	1002	5802	2.9	20.4525	3.9	0.1050	4.0	0.0156	0.6	0.14	99.7	0.6	101.4	3.8	142.7	92.3	99.7	0.6
07SE34-47	IG	1180	3024	1.1	18.1216	13.3	0.1264	13.4	0.0166	0.9	0.07	106.2	1.0	120.9	15.2	419.6	298.8	106.2	1.0
07SE34-48	IG	213	4797	2.9	20.8290	5.6	0.1707	5.9	0.0258	1.8	0.30	164.2	2.9	160.1	8.7	99.7	132.9	164.2	2.9
07SE34-49	IG	1183	9561	2.6	20.6427	2.8	0.1104	3.0	0.0165	0.9	0.32	105.7	1.0	106.3	3.0	120.9	66.0	105.7	1.0
07SE34-50	IG	128	54291	3.4	9.6346	1.4	4.3072	1.5	0.3010	0.6	0.40	1696.1	9.1	1694.7	12.5	1693.0	25.6	1693.0	25.6
07SE34-51	IG	632	7179	2.2	20.5504	5.2	0.1163	5.4	0.0173	1.5	0.28	110.7	1.6	111.7	5.7	131.5	121.3	110.7	1.6
07SE34-52	IG	800	9462	2.7	20.8686	2.4	0.1083	2.8	0.0164	1.3	0.48	104.8	1.4	104.4	2.7	95.2	57.6	104.8	1.4
07SE34-53	IG	1685	16896	3.4	20.6693	2.0	0.1072	2.9	0.0161	2.2	0.74	102.8	2.2	103.4	2.9	117.9	46.3	102.8	2.2
07SE34-54	IG	495	28407	3.1	13.2980	1.6	1.3854	3.1	0.1336	2.7	0.86	808.4	20.5	882.7	18.6	1073.9	32.6	808.4	20.5
07SE34-55	IG	190	3459	2.7	20.0288	13.3	0.1131	13.6	0.0164	2.7	0.20	105.1	2.8	108.8	14.0	191.7	310.5	105.1	2.8
07SE34-56	IG	204	1161	3.1	24.6418	19.8	0.0933	19.9	0.0167	1.8	0.09	106.6	1.9	90.6	17.3	-313.8	512.6	106.6	1.9
07SE34-57	IG	247	13851	0.6	16.9924	1.8	0.7388	3.4	0.0911	2.9	0.86	561.8	15.8	561.7	14.7	561.5	38.2	561.8	15.8
07SE34-58	IG	731	21207	2.9	21.1294	3.1	0.1081	4.0	0.0166	2.6	0.64	105.9	2.7	104.3	4.0	65.8	73.3	105.9	2.7
07SE34-59	IG	1211	12345	2.9	20.7170	2.9	0.1134	3.0	0.0170	0.9	0.31	108.9	1.0	109.1	3.1	112.5	67.5	108.9	1.0
07SE34-60	IG	803	8469	2.8	20.5818	3.2	0.1144	3.3	0.0171	1.0	0.30	109.2	1.1	110.0	3.4	128.0	74.2	109.2	1.1
07SE34-61	IG	369	3969	2.0	21.0505	6.3	0.1095	6.6	0.0167	1.7	0.26	106.9	1.8	105.5	6.6	74.7	150.9	106.9	1.8
07SE34-62	IG	411	5517	3.5	20.9441	5.9	0.1182	6.2	0.0180	1.9	0.31	114.7	2.1	113.4	6.6	86.7	139.0	114.7	2.1
07SE34-63	IG	836	2862	3.2	19.9238	2.8	0.1217	3.1	0.0176	1.4	0.45	112.4	1.6	116.6	3.4	203.8	64.4	112.4	1.6
07SE34-64	IG	108	4785	2.6	21.7939	12.7	0.1875	12.7	0.0296	1.2	0.10	188.2	2.3	174.5	20.4	-8.4	307.0	188.2	2.3
07SE34-65	IG	248	44925	4.4	12.9481	3.6	1.6441	9.4	0.1544	8.7	0.92	925.5	75.1	987.3	59.6	1127.2	72.4	1127.2	72.4
07SE34-66	IG	443	8019	2.6	21.1285	6.0	0.1124	6.0	0.0172	0.6	0.10	110.1	0.6	108.2	6.1	65.9	141.9	110.1	0.6
07SE34-67	IG	123	32241	2.0	10.8198	1.7	3.3389	1.8	0.2620	0.6	0.35	1500.1	8.4	1490.2	14.1	1476.1	32.1	1476.1	32.1
07SE34-68	IG	292	6381	2.1	22.5319	10.8	0.1015	10.9	0.0166	0.9	0.08	106.0	1.0	98.1	10.2	-89.5	266.2	106.0	1.0
07SE34-69	IG	1555	17739	2.0	20.6458	1.3	0.1157	2.0	0.0173	1.5	0.75	110.7	1.6	111.2	2.1	120.6	30.9	110.7	1.6
07SE34-70	IG	353	104184	2.0	10.9486	0.7	3.1799	1.6	0.2525	1.5	0.89	1451.4	19.1	1452.3	12.7	1453.6	14.1	1453.6	14.1
07SE34-71	IG	185	3123	2.5	21.3291	7.8	0.1141	7.9	0.0176	1.3	0.17	112.8	1.5	109.7	8.2	43.3	186.4	112.8	1.5
07SE34-72	IG	273	6522	3.2	20.7578	5.7	0.1116	6.2	0.0168	2.4	0.38	107.4	2.5	107.4	6.3	107.9	135.2	107.4	2.5
07SE34-73	IG	800	12681	2.9	21.1801	3.5	0.1102	3.6	0.0169	0.5	0.14	108.2	0.5	106.1	3.6	60.1	83.9	108.2	0.5
07SE34-74	IG	555	8835	1.8	20.6995	3.0	0.1187	3.7	0.0178	2.1	0.57	113.9	2.4	113.9	4.0	114.5	71.4	113.9	2.4
07SE34-75	IG	169	2550	2.8	20.9426	7.6	0.1124	7.7	0.0171	1.2	0.16	109.1	1.3	108.1	7.9	86.9	181.2	109.1	1.3
07SE34-76	IG	216	2985	1.7	20.7796	6.7	0.1130	6.8	0.0170	1.2	0.17	108.9	1.3	108.7	7.0	105.4	158.3	108.9	1.3
07SE34-77	IG	586	5784	3.1	20.6925	2.3	0.1091	2.5	0.0164	1.1	0.42	104.7	1.1	105.2	2.5	115.3	54.3	104.7	1.1
07SE34-78	IG	761	7290	3.4	20.2841	2.1	0.1659	5.2	0.0244	4.7	0.91	155.4	7.2	155.8	7.5	162.1	49.0	155.4	7.2
07SE34-79	IG	956	13368	3.1	20.6134	2.2	0.1159	3.0	0.0173	2.1	0.68	110.7	2.3	111.3	3.2	124.3	51.9	110.7	2.3
07SE34-80	IG	1266	17070	2.7	20.9474	2.5	0.1108	3.0	0.0168	1.6	0.54	107.6	1.7	106.7	3.0	86.4	59.1	107.6	1.7
07SE34-81	IG	1521	14847	2.1	20.6535	1.6	0.1154	2.1	0.0173	1.3	0.64	110.5	1.4	110.9	2.2	119.8	37.6	110.5	1.4
07SE34-82	IG	672	8784	3.2	20.7386	32.8	0.1090	32.9	0.0164	1.8	0.05	104.8	1.8	105.0	32.8	110.0	794.4	104.8	1.8

Notes:

§CL: Cathodoluminescence; IG: Oscillatory zoned zircon, interpreted to be detrital igneous grain; RXL: Convolute zoning domain, interpreted to be recrystallized zircon; OL: beam overlapped igneous and recrystallized domains.

*Radiogenic

†"Best age" calculated using 206Pb/238U ages for grains younger than 900 Ma and 207Pb/206Pb ages for grains older than 900 Ma.

TABLE DR1. Laser ablation multicollector inductively coupled plasma mass spectrometry U-Pb zircon data. Analyses in which epoxy was overlapped and those with greater than 10% uncertainty, 30% discordance, and/or 5% reverse discordance are excluded. Uncertainties given at 1σ.

07SE34-83	IG	863	4230	3.0	21.1085	5.4	0.1090	5.9	0.0167	2.4	0.40	106.7	2.5	105.0	5.9	68.1	128.7	106.7	2.5
07SE34-84	IG	197	1950	2.2	21.5076	12.4	0.1081	12.5	0.0169	1.7	0.14	107.8	1.8	104.2	12.4	23.4	298.4	107.8	1.8
07SE34-85	IG	538	5511	3.0	20.7713	3.7	0.1225	3.9	0.0185	1.2	0.31	117.9	1.4	117.4	4.4	106.3	88.4	117.9	1.4
07SE34-86	IG	233	3360	2.5	20.8147	12.2	0.1141	12.2	0.0172	0.6	0.05	110.1	0.7	109.7	12.7	101.4	289.3	110.1	0.7
07SE34-87	IG	177	60066	1.4	9.4484	1.1	4.4501	1.6	0.3049	1.2	0.74	1715.8	17.6	1721.7	13.2	1728.9	19.7	1728.9	19.7
07SE34-88	IG	828	11844	2.9	20.9120	2.4	0.1162	2.5	0.0176	0.5	0.20	112.6	0.6	111.6	2.6	90.3	57.6	112.6	0.6
07SE34-89	IG	197	5928	2.4	20.4490	5.2	0.1748	5.5	0.0259	1.7	0.32	165.0	2.8	163.5	8.3	143.2	122.8	165.0	2.8
07SE34-90	IG	923	7164	2.8	21.1420	4.5	0.1054	4.8	0.0162	1.6	0.33	103.4	1.6	101.8	4.6	64.4	107.3	103.4	1.6
07SE34-91	IG	376	2985	1.7	20.5461	5.3	0.1317	5.6	0.0196	1.9	0.34	125.3	2.3	125.6	6.6	132.0	124.2	125.3	2.3
07SE34-92	IG	356	5109	2.2	19.9447	4.5	0.1840	4.7	0.0266	1.2	0.26	169.3	2.0	171.5	7.4	201.4	104.6	169.3	2.0
07SE34-93	IG	458	1716	5.3	20.1108	6.3	0.1085	6.4	0.0158	1.2	0.19	101.2	1.2	104.6	6.4	182.1	146.5	101.2	1.2
07SE34-94	IG	356	5625	2.4	20.7492	4.9	0.1202	5.0	0.0181	0.9	0.18	115.6	1.1	115.3	5.5	108.8	116.6	115.6	1.1
07SE34-95	IG	778	13818	3.3	20.9239	4.1	0.1081	4.3	0.0164	1.5	0.35	104.9	1.6	104.2	4.3	89.0	96.1	104.9	1.6
07SE34-97	IG	522	2865	1.8	20.5125	13.6	0.1332	13.6	0.0198	0.5	0.04	126.5	0.6	127.0	16.2	135.8	320.0	126.5	0.6
07SE34-98	IG	430	6429	2.4	21.1490	4.6	0.1103	4.8	0.0169	1.3	0.27	108.1	1.4	106.2	4.9	63.6	110.7	108.1	1.4
07SE34-99	IG	581	11643	2.8	20.7697	5.2	0.1115	5.8	0.0168	2.4	0.42	107.4	2.6	107.4	5.9	106.5	123.9	107.4	2.6
07SE34-100	IG	709	19890	6.8	19.7216	1.5	0.2219	1.9	0.0317	1.2	0.62	201.4	2.3	203.5	3.5	227.5	33.9	201.4	2.3

1 (originally 08SE467) San Emigdio Schist - San Emigdio Mountains

							Isotope ratios							Apparent ages (Ma)					
Analysis	CL notes[§]	U (ppm)	206Pb 204Pb	U/Th	206Pb* 207Pb*	± (%)	207Pb* 235U*	± (%)	206Pb* 238U	± (%)	error corr.	206Pb* 238U*	± (Ma)	207Pb* 235U	± (Ma)	206Pb* 207Pb*	± (Ma)	Best age† (Ma)	± (Ma)
08SE467-1	IG	965	7478	3.5	21.0049	3.8	0.1363	4.1	0.0208	1.7	0.40	132.5	2.2	129.8	5.0	79.8	89.8	132.5	2.2
08SE467-2	IG	280	3718	2.2	21.3644	6.9	0.1592	7.0	0.0247	1.2	0.17	157.1	1.9	150.0	9.7	39.4	164.5	157.1	1.9
08SE467-3	IG	1534	11970	2.6	21.2329	2.7	0.1198	2.9	0.0185	1.1	0.37	117.9	1.3	114.9	3.2	54.1	64.3	117.9	1.3
08SE467-4	IG	1919	12452	2.3	21.1723	3.2	0.1203	3.9	0.0185	2.2	0.57	118.0	2.6	115.4	4.2	61.0	75.4	118.0	2.6
08SE467-5	IG	761	8394	3.5	20.6891	1.7	0.1246	2.9	0.0187	2.3	0.80	119.4	2.7	119.3	3.3	115.7	41.0	119.4	2.7
08SE467-6	IG	1146	9276	3.9	20.2810	4.1	0.1225	5.5	0.0180	3.6	0.66	115.1	4.1	117.3	6.1	162.5	97.1	115.1	4.1
08SE467-8	RXL	3111	4658	1.8	19.4550	6.8	0.1032	9.3	0.0146	6.3	0.68	93.2	5.8	99.7	8.8	258.9	155.9	93.2	5.8
08SE467-9	IG	904	9838	3.2	19.8595	7.3	0.1280	7.4	0.0184	1.3	0.18	117.8	1.5	122.3	8.5	211.4	168.9	117.8	1.5
08SE467-10	IG	886	5244	3.5	20.8937	3.6	0.1211	4.1	0.0184	1.9	0.48	117.3	2.3	116.1	4.5	92.4	84.8	117.3	2.3
08SE467-11	IG	1060	9172	5.8	20.5317	4.8	0.1303	5.0	0.0194	1.4	0.27	123.9	1.7	124.4	5.9	133.7	113.5	123.9	1.7
08SE467-13	IG	2073	16396	7.4	20.8950	2.2	0.1220	2.3	0.0185	0.8	0.36	118.1	1.0	116.9	2.5	92.3	51.0	118.1	1.0
08SE467-14	IG	1676	9654	1.7	21.0473	2.0	0.1226	2.5	0.0187	1.6	0.63	119.6	1.9	117.5	2.8	75.0	46.9	119.6	1.9
08SE467-15	IG	184	4390	8.1	18.4773	6.0	0.2355	7.2	0.0316	3.9	0.55	200.3	7.8	214.7	13.9	376.0	134.7	200.3	7.8
08SE467-16	RXL	3197	11290	1.6	20.7194	2.2	0.0957	5.8	0.0144	5.4	0.93	92.0	4.9	92.8	5.2	112.2	51.7	92.0	4.9
08SE467-17	IG	642	7842	1.9	20.6723	4.3	0.1614	4.4	0.0242	0.8	0.18	154.1	1.2	151.9	6.2	117.6	102.2	154.1	1.2
08SE467-18	IG	1495	9252	2.0	20.0775	4.9	0.1143	6.1	0.0166	3.6	0.60	106.4	3.8	109.9	6.3	186.0	113.2	106.4	3.8
08SE467-19	IG	1282	10900	14.3	20.9012	2.6	0.1153	3.1	0.0175	1.8	0.56	111.7	1.9	110.8	3.3	91.5	60.6	111.7	1.9
08SE467-20	OL	814	6022	30.1	20.1643	4.2	0.1121	9.0	0.0164	8.0	0.88	104.8	8.3	107.9	9.2	175.9	97.6	104.8	8.3
08SE467-21	IG	172	2226	2.4	20.2952	24.3	0.1088	24.4	0.0160	2.2	0.09	102.4	2.2	104.8	24.3	160.9	576.5	102.4	2.2
08SE467-23	OL	782	8354	38.3	20.9580	5.9	0.1105	5.9	0.0168	0.5	0.08	107.4	0.5	106.4	6.0	85.2	140.6	107.4	0.5
08SE467-24	IG	899	8076	5.6	21.3893	3.4	0.1054	5.6	0.0164	4.5	0.80	104.6	4.6	101.8	5.4	36.6	80.4	104.6	4.6
08SE467-27	IG	2584	8750	4.6	20.5799	2.4	0.1156	2.7	0.0173	1.3	0.49	110.3	1.5	111.1	2.9	128.2	56.0	110.3	1.5
08SE467-28	IG	1955	2756	16.0	16.2838	19.3	0.1383	19.4	0.0163	1.8	0.10	104.4	1.9	131.5	23.9	653.7	417.2	104.4	1.9
08SE467-29	IG	243	2148	3.4	20.4504	17.1	0.1123	17.1	0.0167	1.3	0.07	106.5	1.4	108.1	17.6	143.0	403.2	106.5	1.4
08SE467-30	IG	881	7666	3.2	21.1334	3.5	0.1224	3.7	0.0188	1.4	0.37	119.9	1.6	117.3	4.1	65.3	82.5	119.9	1.6
08SE467-31	IG	284	1944	1.2	21.5657	5.4	0.1438	5.5	0.0225	1.1	0.20	143.4	1.5	136.4	7.0	16.9	128.9	143.4	1.5
08SE467-32	IG	2085	8416	2.6	20.3486	2.8	0.1163	3.8	0.0172	2.5	0.67	109.7	2.7	111.7	4.0	154.7	65.7	109.7	2.7
08SE467-33	IG	591	9114	6.0	21.2713	3.5	0.1197	4.0	0.0185	2.0	0.49	118.0	2.3	114.8	4.4	49.8	83.2	118.0	2.3
08SE467-34	IG	1092	9906	9.4	20.6130	2.8	0.1067	5.4	0.0159	4.6	0.86	102.0	4.7	102.9	5.3	124.3	65.5	102.0	4.7
08SE467-35	IG	357	7976	1.6	18.1155	1.8	0.4314	3.8	0.0567	3.3	0.88	355.4	11.4	364.2	11.5	420.4	40.7	355.4	11.4
08SE467-36	IG	2115	13476	2.0	20.7693	1.4	0.1143	2.9	0.0172	2.5	0.87	110.0	2.7	109.9	3.0	106.5	33.6	110.0	2.7
08SE467-37	IG	2320	7436	6.3	20.3727	2.3	0.1131	7.0	0.0167	6.6	0.95	106.8	7.0	108.8	7.2	151.9	53.5	106.8	7.0
08SE467-39	IG	2173	11298	1.7	21.2314	2.5	0.1144	3.0	0.0176	1.7	0.56	112.6	1.9	110.0	3.1	54.3	59.3	112.6	1.9
08SE467-38	IG	408	11934	11.9	18.9591	2.4	0.3799	2.6	0.0522	1.1	0.42	328.3	3.5	327.0	7.3	317.8	53.9	328.3	3.5
08SE467-42	IG	62	4056	1.8	17.8849	9.0	0.5663	9.2	0.0735	1.8	0.20	457.0	8.1	455.6	33.8	448.9	201.1	457.0	8.1
08SE467-43	IG	1481	10362	2.1	20.8274	2.4	0.1186	2.7	0.0179	1.1	0.42	114.5	1.3	113.8	2.9	99.9	57.3	114.5	1.3
08SE467-44	OL	647	6272	24.0	20.8390	3.6	0.1062	3.7	0.0160	1.1	0.31	102.6	1.2	102.5	3.6	98.6	84.2	102.6	1.2
08SE467-45	IG	1175	9090	3.7	20.8822	1.7	0.1143	3.1	0.0173	2.6	0.84	110.7	2.8	109.9	3.2	93.7	39.5	110.7	2.8
08SE467-46	IG	903	6758	3.1	20.9220	2.3	0.1211	2.4	0.0184	0.5	0.21	117.3	0.6	116.0	2.6	89.2	55.2	117.3	0.6
08SE467-47	IG	1138	7490	3.9	20.6873	1.3	0.1276	1.6	0.0191	0.9	0.57	122.2	1.1	121.9	1.8	115.9	30.7	122.2	1.1
08SE467-48	IG	1087	7534	2.6	21.0042	4.3	0.1234	4.7	0.0188	1.9	0.40	120.1	2.2	118.2	5.2	79.9	102.1	120.1	2.2
08SE467-49	IG	935	5584	6.5	20.6227	3.1	0.1153	3.3	0.0172	1.3	0.38	110.2	1.4	110.8	3.5	123.2	72.9	110.2	1.4
08SE467-50	IG	205	1878	15.1	23.3931	11.9	0.0996	12.0	0.0169	0.7	0.06	108.0	0.7	96.4	11.0	-182.3	299.2	108.0	0.7
08SE467-51	IG	1952	14714	4.5	20.4508	2.8	0.1080	4.9	0.0160	4.0	0.81	102.5	4.0	104.2	4.8	143.0	66.4	102.5	4.0
08SE467-52	RXL	2411	4148	11.3	18.9007	8.4	0.1113	8.4	0.0153	1.3	0.15	97.6	1.2	107.2	8.6	324.9	189.9	97.6	1.2
08SE467-53	IG	2886	10868	9.5	18.6062	8.0	0.1274	8.5	0.0172	2.7	0.32	109.9	3.0	121.8	9.7	360.4	181.7	109.9	3.0
08SE467-54	IG	1995	13986	6.5	20.8500	2.2	0.1178	2.5	0.0178	1.1	0.44	113.8	1.2	113.1	2.6	97.4	52.0	113.8	1.2
08SE467-55	IG	2005	10568	2.5	20.7271	5.9	0.1053	8.1	0.0158	5.5	0.68	101.3	5.5	101.7	7.8	111.4	139.2	101.3	5.5
08SE467-56	IG	1576	10104	2.8	20.7695	2.8	0.1195	3.4	0.0180	1.9	0.57	115.0	2.2	114.6	3.7	106.5	65.5	115.0	2.2
08SE467-57	OL	2476	6228	53.2	20.0714	3.5	0.1133	3.6	0.0165	1.2	0.32	105.4	1.2	108.9	3.8	186.7	80.5	105.4	1.2
08SE467-58	IG	219	2280	10.6	21.4431	4.7	0.1404	8.2	0.0218	6.7	0.82	139.2	9.2	133.4	10.2	30.6	113.9	139.2	9.2
08SE467-59	OL	2802	13994	24.1	20.4315	1.3	0.1250	1.5	0.0185	0.9	0.57	118.3	1.0	119.6	1.7	145.1	29.7	118.3	1.0
08SE467-60	IG	183	1862	11.0	18.1111	24.7	0.1709	25.0	0.0224	4.0	0.16	143.1	5.7	160.2	37.0	420.9	558.0	143.1	5.7
08SE467-61	IG	1566	10430	6.4	20.6625	1.3	0.1195	2.4	0.0179	2.0	0.83	114.4	2.3	114.6	2.6	118.7	31.7	114.4	2.3
08SE467-62	IG	927	6398	6.0	20.6886	3.2	0.1264	3.4	0.0190	0.9	0.26	121.1	1.0	120.8	3.8	115.8	76.5	121.1	1.0
08SE467-63	IG	2790	10196	2.5	20.3865	2.1	0.1200	3.4	0.0177	2.7	0.79	113.4	3.0	115.1	3.7	150.3	48.8	113.4	3.0
08SE467-65	IG	992	16270	8.0	19.7121	1.7	0.1981	2.5	0.0283	1.8	0.74	180.1	3.3	183.6	4.2	228.6	39.0	180.1	3.3
08SE467-66	IG	1103	7526	11.7	21.0548	3.8	0.1144	4.6	0.0175	2.6	0.55	111.7	2.8	110.0	4.8	74.2	91.2	111.7	2.8
08SE467-67	IG	190	1380	2.7	24.5385	16.0	0.0934	16.1	0.0166	1.8	0.11	106.3	1.9	90.6	14.0	-303.0	411.5	106.3	1.9
08SE467-68	IG	922	6984	5.6	20.4619	3.5	0.1238	5.7	0.0184	4.5	0.79	117.4	5.2	118.5	6.4	141.7	82.7	117.4	5.2
08SE467-69	IG	1562	2478	3.9	18.7951	6.1	0.1326	6.1	0.0181	0.7	0.11	115.5	0.8	126.5	7.3	337.6	138.3	115.5	0.8
08SE467-70	IG	410	2286	2.0	21.7687	6.6	0.1141	6.7	0.0180	0.6	0.09	115.1	0.7	109.7	6.9	-5.6	160.2	115.1	0.7
08SE467-71	IG	1139	9142	16.2	20.9853	1.6	0.1109	3.0	0.0169	2.6	0.85	107.9	2.7	106.8	3.0	82.0	36.9	107.9	2.7
08SE467-72	IG	1497	3326	6.9	17.3723	12.5	0.1790	13.2	0.0226	4.3	0.33	143.8	6.1	167.2	20.3	513.1	274.8	143.8	6.1
08SE467-73	IG	1521	8862	4.2	20.6971	1.5	0.1148	4.0	0.0172	3.7	0.93	110.1	4.1	110.4	4.2	114.7	35.0	110.1	4.1
08SE467-74	IG	1947	10910	4.4	20.3079	3.9	0.1191	4.1	0.0175	1.3	0.31	112.1	1.4	114.3	4.5	159.4	91.9	112.1	1.4
08SE467-75	IG	2661	1470	12.6	17.1410	8.9	0.1400	8.9	0.0174	0.9	0.10	111.2	0.9	133.0	11.1	542.5	194.8	111.2	0.9
08SE467-1b	IG	1351	3806	3.9	23.6818	13.4	0.0963	17.3	0.0165	10.9	0.63	105.8	11.4	93.4	15.4	-213.0	337.6	105.8	11.4
08SE467-3b	RXL	2944	3951	28.9	21.0166	6.2	0.0935	6.9	0.0142	3.0	0.44	91.2	2.7	90.7	6.0	78.5	146.6	91.2	2.7
08SE467-4b	IG	471	1198	2.9	23.5797	18.0	0.0990	19.0	0.0169	6.3	0.33	108.2	6.7	95.9	17.4	-202.1	454.0	108.2	6.7

Notes:
§CL: Cathodoluminescence; IG: Oscillatory zoned zircon, interpreted
to be detrital igneous grain; RXL: Convolute zoning domain, interpreted to be recrystallized zircon; OL: beam overlapped igneous and recrystallized domains.
*Radiogenic
†"Best age" calculated using 206Pb/238U ages for grains younger than 900 Ma and 207Pb/206Pb ages for grains older than 900 Ma.

TABLE DR2. SIMS zircon oxygen isotope data.

3 (originally 06SE23) San Emigdio Schist - San Emigdio Mountains

Analysis	CL notes§	Measured $^{18}O/^{16}O$ ($x10^{-3}$)	± ($x10^{-3}$)*	$\delta^{18}O_{VSMOW}$ (‰)	± (‰)*	U-Pb age (Ma)†	± (Ma)*
06SE23_det1IG.asc	IG	2.0099	0.000428	5.2	0.4	966.0	32.7
06SE23_det1b.asc	IG	2.0112	0.000817	5.5	0.5	105.0	1.8
06SE23_det1MM2.asc	RXL	2.0136	0.000900	6.3	0.5	99.3	0.9
06SE23_2.asc	RXL	2.0162	0.001026	7.3	0.6	nd	nd

1 (originally 08SE467) San Emigdio Schist - San Emigdio Mountains

Analysis	CL notes§	Measured $^{18}O/^{16}O$ ($x10^{-3}$)	± ($x10^{-3}$)*	$\delta^{18}O_{VSMOW}$ (‰)	± (‰)*	U-Pb age (Ma)†	± (Ma)*
08SE467_1.asc	IG	2.0230	0.000785	6.3	0.8	nd	nd
08SE467_2.asc	IG	2.0214	0.000750	5.6	0.8	157.1	1.9
08SE467_8.asc	IG	2.0237	0.001382	6.8	1.0	nd	nd
08SE467_9.asc	IG	2.0236	0.000921	6.9	0.8	nd	nd
08SE467_9.asc	IG	2.0212	0.000461	5.8	0.7	119.4	2.7
08SE467_9b.asc	IG	2.0213	0.000576	5.9	0.7	119.4	2.7
08SE467_12.asc	IG	2.0209	0.000590	5.8	0.7	118.0	2.6
08SE467_12b.asc	IG	2.0195	0.000583	5.2	0.7	118.0	2.6
08SE467_14.asc	IG	2.0194	0.000920	5.3	0.8	108.2	6.7
08SE467_14.asc	IG	2.0194	0.000836	5.4	0.7	123.9	1.7
08SE467_14MM.asc	RXL	2.0238	0.000738	7.7	0.7	91.2	0.7
08SE467_14MM2.asc	RXL	2.0233	0.001028	7.5	0.8	93.2	5.8
08SE467_15.asc	RXL	2.0222	0.000635	7.1	0.6	91.2	2.7
08SE467_23.asc	OL	2.0212	0.000900	6.7	0.7	105.4	1.2
08SE467_25.asc	OL	2.0204	0.001128	6.4	0.8	102.6	1.2
08SE467_31.asc	RXL	2.0226	0.001040	7.6	0.7	97.6	1.2
08SE467_32.asc	RXL	2.0218	0.000910	7.3	0.7	92.0	4.9

7 (originally 08SE46) San Emigdio tonalite - San Emigdio Mountains

Analysis	CL notes§	Measured $^{18}O/^{16}O$ ($x10^{-3}$)	± ($x10^{-3}$)*	$\delta^{18}O_{VSMOW}$ (‰)	± (‰)*	U-Pb age (Ma)†	± (Ma)*
08SE46_1.asc	IG	2.0203	0.001275	4.8	0.7	133.1	3.6
08SE46_1b.asc	RXL	2.0287	0.001408	9.0	0.8	100.7	2.5
08SE46_1c.asc	RXL	2.0252	0.001473	7.2	0.8	102.3	3.7
08SE46_1d.asc	IG	2.0232	0.000995	6.2	0.6	144.8	7.3
08SE46_2.asc	IG	2.0230	0.001921	6.1	1.0	153.0	4.1
08SE46_3.asc	IG	2.0209	0.000775	5.1	0.5	130.3	5.3
08SE46_3b.asc	RXL>OL	2.0251	0.000887	7.1	0.6	104.5	1.8
08SE46_4.asc	IG	2.0204	0.000750	4.8	0.5	143.3	3.4
08SE46_4b.asc	RXL>OL	2.0246	0.000731	6.9	0.5	104.5	2.8
08SE46_5.asc	IG	2.0198	0.000978	4.5	0.6	145.8	3.9
08SE46_5b.asc	RXL	2.0233	0.000815	6.3	0.6	103.5	4.6
08SE46_19.asc	IG	2.0155	0.000705	6.0	0.5	159.4	7.2
08SE46_20.asc	IG	2.0160	0.000546	6.3	0.5	145.3	3.8
08SE46_21.asc	IG	2.0146	0.000676	5.6	0.5	150.2	2.8
08SE46_21b.asc	IG	2.0151	0.000778	5.9	0.6	132.8	2.6
08SE46_22.asc	IG	2.0138	0.000765	5.2	0.6	133.6	4.9
08SE46_23.asc	IG	2.0143	0.000636	5.4	0.5	134.5	2.8

Notes:
§CL: Cathodoluminescence; IG: Oscillatory zoned zircon, interpreted to be detrital igneous grain; RXL: Convolute zoning domain, interpreted to be recrystallized zircon; OL: beam overlapped igneous and recrystallized domains.
*Uncertainties given at 2σ.
†Corresponding 206Pb/238U ages determined within the same crystal growth domain; nd, not determined.

TABLE DR2. SIMS zircon oxygen isotope data.

08SE46_24.asc	IG	2.0150	0.000770	5.8	0.6	140.8	3.7
08SE46_25.asc	IG	2.0132	0.001239	4.9	0.7	136.1	5.6
08SE46_26.asc	IG	2.0148	0.000851	5.7	0.6	135.9	3.2
08SE46_27.asc	IG	2.0151	0.000616	5.8	0.5	131.1	1.4
08SE46_28.asc	IG	2.0135	0.000469	5.0	0.5	134.1	4.7
08SE46_29.asc	IG	2.0148	0.000758	5.7	0.6	131.5	3.2
08SE46_30.asc	IG	2.0145	0.000877	5.5	0.6	136.8	2.3
08SE46_31.asc	IG	2.0144	0.000690	5.5	0.5	137.7	3.8

8 (originally 08SE675) San Emigdio tonalite - San Emigdio Mountains

Analysis	CL notes§	Measured $^{18}O/^{16}O$ ($x10^{-3}$)	± ($x10^{-3}$)*	$\delta^{18}O_{VSMOW}$ (‰)	± (‰)*	U-Pb age (Ma)†	± (Ma)*
08SE675_det1a.asc	IG	2.0159	0.000424	5.8	0.5	133.6	3.4
08SE675_det1b.asc	IG	2.0161	0.000750	6.1	0.6	133.6	3.4
08SE675_det2a.asc	IG	2.0142	0.000636	5.2	0.5	135.5	4.3
08SE675_det2b.asc	RXL	2.0171	0.000713	6.8	0.5	98.2	1.7
08SE675_det3a.asc	IG	2.0128	0.000641	4.7	0.5	132.6	4.6
08SE675_det3b@1.asc	OL	2.0146	0.000742	5.6	0.5	116.1	9.1
08SE675_det4a.asc	IG	2.0123	0.000715	5.1	0.5	134.4	4.2
08SE675_det4c.asc	RXL	2.0135	0.000500	6.7	0.5	95.8	6.3
08SE675_5.asc	IG	2.0168	0.000494	4.7	0.5	140.4	4.2
08SE675_6.asc	IG	2.0151	0.000667	4.5	0.4	137.3	7.4
08SE675_7.asc	IG	2.0148	0.000507	5.3	0.5	144.3	3.8

Notes:
§CL: Cathodoluminescence; IG: Oscillatory zoned zircon, interpreted
to be detrital igneous grain; RXL: Convolute zoning domain, interpreted to be recrystallized zircon; OL: beam overlapped igneous and recrystallized domains.
*Uncertainties given at 2σ.
†Corresponding 206Pb/238U ages determined within the same crystal growth domain; nd, not determined.